Atomic scale investigation of dynamic precipitation and grain boundary segregation in a 6061 aluminium alloy nanostructured by ECAP

X. Sauvage[1]*, M. Yu. Murashkin[2], R. Z. Valiev[2]

[1] *Université de Rouen, Groupe de Physique des Matériaux, UMR CNRS 6634, BP 12, 76801 Saint-Etienne du Rouvray, France*
[2] *Institute of Physics of Advanced Materials, Ufa State Aviation Technical University, K. Marx 12, Ufa 450000, Russia*

Received 10 September 2010, received in revised form 16 September 2010, accepted 17 September 2010

Abstract

A commercial 6061 aluminium alloy was processed by ECAP and subsequently aged to nucleate nanoscaled precipitates within the ultrafine grain structure. The mechanical behaviour was investigated thanks to tensile tests and the microstructure was characterized at the atomic scale using Atom Probe Tomography. These experimental data clearly reveal that extensive dynamic precipitation and grain boundary segregation occurred during ECAP. These features lead to a significant increase of the strength of the alloy. Further ageing after ECAP processing gives rise to an additional increase of the strength linked to a larger precipitate density. A comparison of the morphology and the composition of precipitates nucleated during ECAP and during the standard T6 ageing treatment shows that the precipitation kinetic is affected by the severe plastic deformation.

Key words: aluminium alloy, precipitation, grain boundary segregation, ECAP

1. Introduction

During the last decade, severe plastic deformation (SPD) techniques have been successfully applied to a large number of metallic alloys to achieve ultrafine-grained structures with unique properties [1, 2]. Thanks to the refinement of coarse-grained structures down to the nanoscale, high strength and superplastic properties are commonly achieved in light alloys. Among commercial aluminium alloys, the age hardenable 6061 is widely used because it exhibits a good combination of formability, strength, corrosion resistance and weldability [3–6]. To further increase the strength of this alloy, some authors proposed to combine nanostructuring by SPD using equal channel angular pressing (ECAP) and precipitation by post-ECAP ageing treatment [7–10]. This approach is extremely interesting because a fine distribution of precipitates in a bulk nanostructured material may increase both the yield stress but also the ductility [11, 12]. Several authors have applied this approach for various aluminium alloys [7, 9, 13–16], but controlling the precipitation kinetics in SPD metals is a critical issue because there might be a competition between recovery, recrystallization and grain growth, while heterogeneous precipitation along dislocations and/or grain boundaries is very likely to occur [17]. It is also interesting to note that in such a situation a fastest precipitation kinetic was sometime reported and some of the classical metastable phases do not longer appear [18]. Moreover, some recent experimental investigations have clearly shown that during SPD some grain boundary segregation may occur [19, 20], and such features may also affect the precipitation kinetics.

The aim of this study was to apply the Atom Probe Tomography (APT) technique to point out the evolution of the distribution of the alloying elements in a 6061 commercial alloy during ECAP processing and after subsequent ageing. A special emphasis was given on the nucleation of nanoscaled precipitates and the

*Corresponding author: tel.: + 33 2 32 95 51 42; fax: + 33 2 32 95 50 32; e-mail address: xavier.sauvage@univ-rouen.fr

formation of grain boundary segregations with a link to the mechanical properties.

2. Experimental

The material investigated in the present study is a commercial 6061 aluminium alloy (Mg 0.8–1.2, Si 0.4–0.8, Cu 0.15–0.4, Cr 0.15–0.35, Mn 0.15, Fe 0.7, Zn 0.25, Ti 0.15 (wt.%), Al balance).

Billets (20 mm in diameter and 150 mm in length) of the as-received material were solution treated at 530 ℃ during one hour and then water quenched in ice brine. The solution treated material exhibits equiaxed grains with a mean size of about 100 μm. Then, billets were processed by ECAP: four passes at 110 ℃ following the route Bc with a die angle of 90° and an extrusion speed of 10 mm s^{-1} (samples referred as ECAP). After ECAP processing, part of the billets were aged at 130 ℃ during 24 h (samples referred as ECAP + ageing). For comparison, a piece of the solution treated but non-deformed material was subjected to the standard T6 ageing treatment: 170 ℃ during 12 h (samples referred as T6).

Tensile tests were performed at room temperature on specimens (gauge length 11 mm, section 1 × 2.5 mm^2) cut along the longitudinal direction of the ECAP billet. Experiments were carried out on a tensile testing machine (INSTRON 1185) controlled under constant cross-head speed condition with an initial strain rate of 1.8×10^{-3} s^{-1}.

To investigate the distribution of alloying elements and more especially nanoscaled precipitates, the material was analysed by APT. Samples were prepared by standard electropolishing techniques and then analysed at a temperature of 50 K in UHV conditions using electric pulses (16 % pulse fraction and 2 kHz repetition rate). Data processing was performed using the GPM 3D Data software®.

3. Results and discussion

The tensile behaviour of the 6061 aluminium of the present study was recorded in three different states: (i) T6 treated, (ii) solution treated and ECAP processed, (iii) solution treated, ECAP processed and additionally aged during 24 h at 130 ℃ (Fig. 1). It is interesting to note that the yield stress of the ECAPed material is significantly higher than the yield stress of the T6 treated alloy (400 vs 275 MPa) but the uniform elongation is strongly reduced (4.5 % vs 11 %) which is a rather common feature for SPD materials. The ageing treatment performed after ECAP processing leads to further increase of the yield stress (up to 430 MPa) and also a small improvement of the ductility (up to 5 % uniform elongation). This treatment was performed to nucleate some nanoscaled precipitates and to combine grain boundary together with precipitation hardening, thus the increase of strength was expected. It should be noted however that it is not as large as usually observed in the coarse grained 6061 alloy (typically about 120 MPa) and this feature will be discussed later on the basis of microstructural observations. Another interesting point is the larger strain hardening rate that obviously appears on the stress-strain curve.

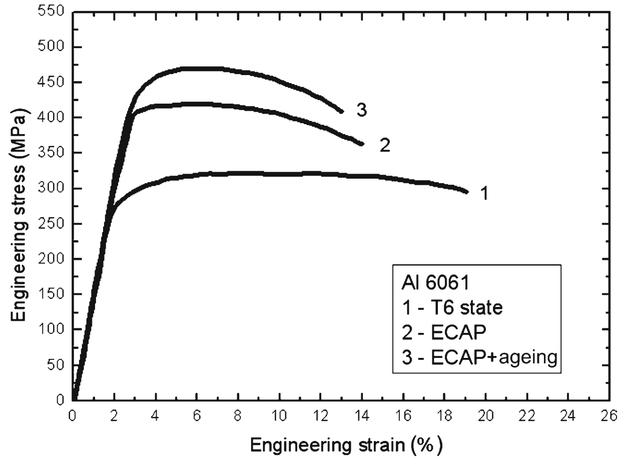

Fig. 1. Stress-strain plot of the 6061 aluminium alloy T6 treated, processed by ECAP in the solution treated state and processed by ECAP followed by additional ageing.

For a better understanding of the evolution of the mechanical behaviour during these various combinations of thermal treatment and SPD processing, the material was characterized by APT with a special emphasis on Mg rich precipitates that are known to be responsible of the age hardening behaviour of 6061 aluminium alloys [3–6]. For a better visualisation of these precipitates, data were filtered to exhibit only Mg, Cu and Si atoms located in regions containing more than 5 at.% Mg (see details of the procedure in [21]). The T6 treated alloy exhibits a high density of needle shape precipitates containing Mg, Si and Cu (Fig. 2). It has been shown by other authors that these precipitates are aligned along the (001) direction of the fcc lattice of the aluminium matrix [4, 5] and that they are meta-stable phases (called β'') with a composition different from the stable Mg_2Si phase [3]. In the present T6 treated material, APT data show that these needle shape precipitates have a diameter of about 3 nm with an aspect ratio in a range of 2 to 3. They contain between 12 and 20 at.% Mg while the copper concentration is in a range of 1 to 2 at.%. The Mg/Si ratio was measured close to 1.5, in agreement with data reported by Murayama and co-authors [3].

ECAP processing was performed in the solid solution state, i.e. where alloying elements (Mg, Si and Cu) are in solid solution (APT data of the solution

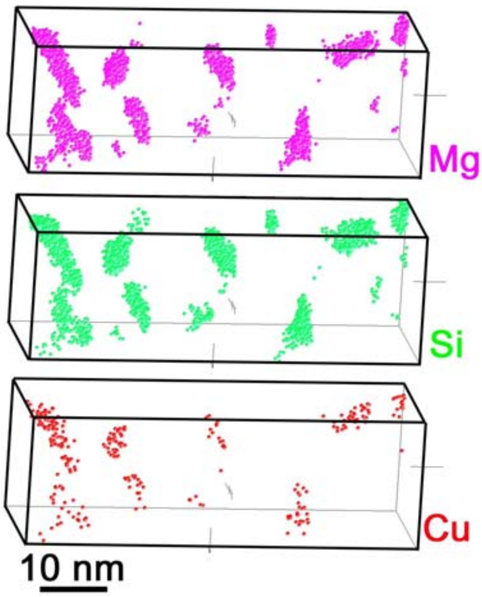

Fig. 2. 3D reconstruction ($20 \times 20 \times 60$ nm^3) of a volume analysed in the T6 treated 6061 aluminium alloy. The data set was filtered to exhibit Mg rich nanoscaled precipitates. The distribution of Mg, Si and Cu is displayed on three different images.

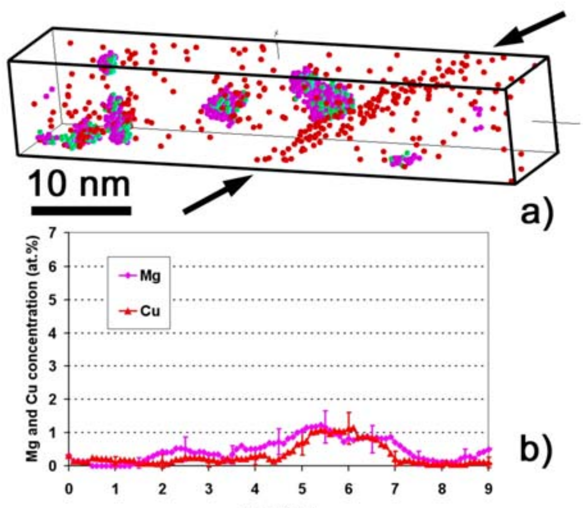

Fig. 3. (a) 3D reconstruction ($10 \times 10 \times 55$ nm^3) of a volume analysed in the 6061 aluminium alloy processed by ECAP. The data set was filtered to exhibit Mg rich nanoscaled precipitates (Mg pink, Si green and Cu red). Additionally, all Cu atoms detected in the volume are plotted to show segregation along a planar boundary (arrowed); (b) composition profile computed across this boundary showing a significant segregation of Cu and Mg (sampling volume thickness 1 nm).

treated state are not shown here). However, surprisingly the 3D reconstruction of the volume analysed in

Table 1. Diffusion coefficient (D) of Mg in Al calculated for the ECAP temperature (T = 110 ℃), the T6 treatment temperature (T = 170 ℃) and the post-ECAP ageing temperature (T = 130 ℃) from [24]; mean diffusion length ($L = (6Dt)^{1/2}$) estimated for the duration (t) of the ECAP processing and ageing treatments

T (℃)	D (10^{-22} m^2 s^{-1})	t (h)	L (nm)
110	5.5	0.5	2
130	36	24	43
170	927	12	155

the ECAPed material clearly reveals that there is a significant volume fraction of nanoscaled precipitates (Fig. 3a). These precipitates, however, exhibit a different morphology comparing to the T6 state. They are not needle shape but spherical, with an average diameter of about 3 nm. They contain a similar amount of Mg (in a range of 12 to 20 at.%) and Cu (in a range of 1 to 2 at.%) but a higher Mg/Si ratio which is about 2 instead of 1.5 for the T6 state. This latter feature is typical for the metastable β' phase [3]. Thus, it seems that during SPD the dynamic precipitation process does not involve the β'' phase observed in the standard T6 ageing treatment. Roven and co-authors have also reported some dynamic precipitation in a similar alloy processed by ECAP [15]. They observed some spherical precipitates by TEM, but without analytical measurement they attributed them to the β'' phase. It should be also noted that dynamic precipitation during SPD in such Al alloy was also reported during high ratio differential speed rolling [22]. The different morphology (sphere vs needle shape for T6 conventional treatment) might be attributed to the strong dislocation activity during ECAP processing and the resulting shear of precipitates. Murayama and co-authors have even shown that this phenomenon may lead to the complete dissolution of existing precipitates [23].

Another interesting feature exhibited in the reconstructed volume displayed in the Fig. 3a is a Cu planar segregation. For more clarity, on this image only Mg atoms located in clusters are displayed (filtering procedure) but all Cu atoms are plotted. However, there is also a significant amount of Mg in this Cu rich layer, as shown on the composition profile computed across it (Fig. 3b). In this 2 nm thick layer, Cu and Mg enrichment are roughly similar, up to 1 at.%. As reported in recent studies, this feature might be attributed to some SPD induced grain boundary segregation [19, 20].

Considering the low temperature during ECAP (110 ℃) and the short time of the processing (billet held at this temperature not more than 30 min), the nucleation of precipitates and also the grain boundary segregation during SPD were absolutely not expected. Indeed, as shown in Table 1, in such conditions the

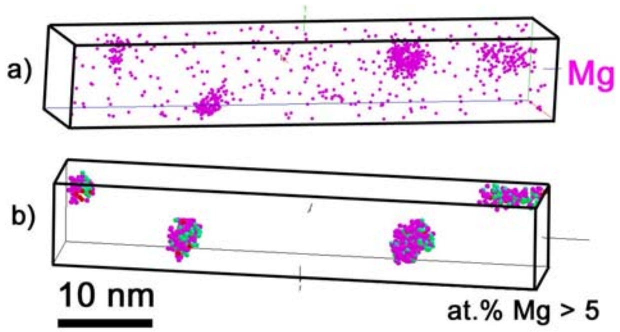

Fig. 4. 3D reconstruction ($10 \times 10 \times 60\ nm^3$) of a volume analysed in the 6061 aluminium alloy processed by ECAP followed by ageing during 24 h at 130 ℃. (a) Distribution of all detected Mg atoms showing nanoscaled spherical precipitates; (b) filtered data with another orientation (Mg atoms pink, Si atoms green and Cu atoms red).

atomic mobility is extremely limited and obviously the thermal diffusion cannot account for the observed phenomena. Thus, as already proposed in earlier studies [19, 20, 25, 26], the atomic mobility was most probably promoted by defects like dislocations (via solute drag or pipe diffusion [27]) or SPD induced vacancies [25].

Of course, the high density of nanoscaled precipitates may significantly affect the mechanical behaviour and one may conclude that the high yield stress recorded for the ECAP state (Fig. 1) is the result of a combination of grain boundary strengthening (ultrafine grain structure created during SPD) and precipitation hardening. The high density of precipitates observed for this state may also explain the relatively high elongation to failure measured after ECAP (about 6 %), which is usually only few percents after SPD in aluminium alloys. As proposed by other authors, the precipitates act as additional dislocation sources which increase the ductility [11–13]. The observed grain boundary segregations may also affect the properties of the ultrafine grained alloy; however this point is still under debate [20].

After ECAP, the material was further aged at 130 ℃ during 24 h. As shown in Table 1, in such conditions, the atomic mobility is high enough to promote more phase separation. Indeed, after ECAP, the concentration of solute element in the fcc Al matrix is still higher than the equilibrium (0.46 ± 0.05 at.% Mg). This indicates that there is some driving force left for the nucleation of new precipitates or for the growth of already existing ones. The precipitates that were analysed in the material processed by ECAP followed by ageing (Fig. 4) are very similar to those observed directly after ECAP (Fig. 3). They are still spherical with an average diameter of about 3 nm and their composition did not significantly change. Due to the small analysed volumes, it is impossible to provide an accurate precipitate density, however it is important to note that the Mg concentration in the fcc Al matrix significantly decreased during this ageing at 130 ℃ during 24 h (down to 0.3 ± 0.05 at.% Mg), indicating that further precipitation occurred. As observed on stress-strain curves (Fig. 1), this leads to a significant increase of the yield stress and of the strain hardening rate, and in a smaller proportion of the uniform elongation. However, since most of the precipitation occurred during the ECAP processing, the additional increase of yield stress resulting from subsequent ageing at 130 ℃ during 24 h is rather small (much smaller than in the non-deformed alloy).

4. Conclusions

(i) A commercial 6061 aluminium alloy in the solutionized state was successfully processed by ECAP at 110 ℃.

(ii) After ECAP, the yield stress is higher than after a standard T6 ageing treatment but the ductility is significantly lower.

(iii) APT analyses demonstrated that some dynamic precipitation and grain boundary segregation occurred during ECAP.

(iv) Considering the low temperature and the short time of the ECAP processing, it is believed that the precipitation and the grain boundary segregation are promoted by an enhanced atomic mobility resulting from SPD induced vacancies and pipe diffusion along dislocations.

(v) It was found that during ECAP, nanoscaled spheres of β' phase nucleate while during the standard T6 ageing treatments needle shape β'' precipitates were observed.

(vi) Ageing treatment performed after the ECAP processing leads to a further increase of strength linked to some additional precipitation.

Acknowledgement

G. Nurislamova is gratefully acknowledged for her contribution to APT analyses.

References

[1] VALIEV, R. Z.—ISLAMGALIEV, R. K.—ALEXANDROV, I. V.: Prog. Mat. Sci., *45*, 2000, p. 103. doi:10.1016/S0079-6425(99)00007-9

[2] VALIEV, R. Z.—LANGDON, T. G.: Prog. Mater. Sci., *51*, 2006, p. 881. doi:10.1016/j.pmatsci.2006.02.003

[3] MURAYAMA, M.—HONO, K.—SAGA, M.—KIKUCHI, M.: Mater. Sci. Eng., *A 250*, 1998, p. 127. doi:10.1016/S0921-5093(98)00548-6

[4] EDWARDS, G. A.—STILLER, K.—DUNLOP, G. L.—COUPER, M. J.: Acta Mater., *46*, 1998, p. 3893. doi:10.1016/S1359-6454(98)00059-7
[5] ANDERSEN, S. J.—ZANDBERGEN, H. W.—JANSEN, J.—TRÆHOLT, C.—TUNDAL, U.—REISO, O.: Acta Mater., *46*, 1998, p. 3283. doi:10.1016/S1359-6454(97)00493-X
[6] DE GEUSER, F.—LEFEBVRE, W.—BLAVETTE, D.: Philos. Mag. Letters, *86*, 2006, p. 227. doi:10.1080/09500830600643270
[7] KIM, W. J.—KIM, J. K.—PARK, T. J.—HONG, S. I.—KIM, D. I.—KIM, Y. S.—LEE, J. D.: Metall. Mater. Trans., *A 33*, 2002, p. 3155. doi:10.1007/s11661-002-0301-4
[8] KIM, J. K.—JEONG, H. G.—HONG, S. I.—KIM, Y. S.—KIM, W. J.: Scripta Mater., *45*, 2001, p. 901. doi:10.1016/S1359-6462(01)01109-5
[9] KIM, J. K.—KIM, H. K.—PARK, J. W.—KIM, W. J.: Scripta Mater., *53*, 2005, p. 1207. doi:10.1016/j.scriptamat.2005.06.014
[10] KIM, W. J.—WANG, J. Y.: Mater. Sci. Eng., *A 464*, 2007, p. 23. doi:10.1016/j.msea.2007.03.074
[11] CHENG, S.—ZHAO, Y. H.—ZHU, Y. T.—MA, E.: Acta Mater., *55*, 2007, p. 5822.
[12] MA, E. : JOM, *58*, 2006, p. 49.
[13] ZHAO, Y. H.—LIAO, X. Z.—JIN, Z.—VALIEV, R. Z.—ZHU, Y. T.: Acta Mater., *52*, 2004, p. 4589. doi:10.1016/j.actamat.2004.06.017
[14] SHA, G.—WANG, Y. B.—LIAO, X. Z.—DUAN, Z. C.—RINGER, S. P.—LANGDON, T. G.: Acta Mater., *57*, 2009, p. 3123. doi:10.1016/j.actamat.2009.03.017
[15] ROVEN, H. J.—LIU, M.—WERENSKIOLD, J. C.: Mat. Sci. Eng., *A 483–484*, 2008, p. 54. doi:10.1016/j.msea.2006.09.142
[16] MURASHKIN, M. YU.—BOBRUK, E. V.—KIL'MAMETOV, A. R.—VALIEV, R. Z.: Phys. Met. Metall., *108*, 2009, p. 415. doi:10.1134/S0031918X09100123
[17] CERRI, A.—LEO, P.: Mat. Sci. Eng., *A 410–411*, 2005, p. 226. doi:10.1016/j.msea.2005.08.135
[18] CIZEK, J.—PROCHAZKA, I.—SMOLA, B.—STULIKOVA, I.—KUZEL, R.—MATEJ, Z.—CHERKASKA, V.—ISLAMGALIEV, R. K.—KULYASOVA, O.: Mater. Sci. Forum, *503–504*, 2006, p. 149.
[19] NURISLAMOVA, G.—SAUVAGE, X.—MURASHKIN, M. YU.—ISLAMGALIEV, R.—VALIEV, R. Z.: Philos. Mag. Lett., *88*, 2008, p. 459. doi:10.1080/09500830802186938
[20] VALIEV, R. Z.—ENIKEEV, N. A.—MURASHKIN, M. YU.—KAZYKHANOV, V. U.—SAUVAGE, X.: Scripta Mater., *63*, 2010, p. 949. doi:10.1016/j.scriptamat.2010.07.014
[21] SAUVAGE, X.—DA COSTA, G.—VALIEV, R. Z.: Ultrafine Grained Materials III. Pennsylvania, TMS – Warrendale 2004, p. 31.
[22] KIM, W. J.—WANG, J. Y.—CHOI, S. O.—CHOI, H. J.—SOHN, H. T.: Mater. Sci. Eng., *A 520*, 2009, p. 23. doi:10.1016/j.msea.2009.05.010
[23] MURAYAMA, M.—HORITA, Z.—HONO, K.: Mater. Trans. JIM, *40*, 1999, p. 938.
[24] DU, Y.—CHANG, Y. A.—HUANG, B.—GONG, W.—JIN, A.—XU, H.—YUAN, Z.—HE, Y.—XIE, F.-Y.: Mater. Sci. Eng., *A 363*, 2003, p. 140. doi:10.1016/S0921-5093(03)00624-5
[25] QUELENNEC, X.—MENAND, A.—LE BRETON, J. M.—PIPPAN, R.—SAUVAGE, X.: Philos. Mag., *90*, 2010, p. 1179. doi:10.1080/14786430903313682
[26] SAUVAGE, X.—CHBIHI, A.—QUELENNEC, X.: Journal of Physics: Conference Series, *240*, 2010, p. 012003.
[27] PICU, R. C.—ZHANG, D.: Acta Mater., *52*, 2004, p. 161. doi:10.1016/j.actamat.2003.09.002